JVI Journals.ASM.org

Human T-Cell Leukemia Virus Type 1 Tax-Deregulated Autophagy Pathway and c-FLIP Expression Contribute to Resistance against Death Receptor-Mediated Apoptosis

Weimin Wang, Jiansuo Zhou, Juan Shi, Yaxi Zhang, Shilian Liu, Yanxin Liu, Dexian Zheng

National Laboratory of Medical Molecular Biology, Institute of Basic Medical Sciences, Chinese Academy of Medical Sciences and Peking Union Medical College, Beijing, China

ABSTRACT

The human T-cell leukemia virus type 1 (HTLV-1) Tax protein is considered to play a central role in the process that leads to adult T-cell leukemia/lymphoma (ATL) and HTLV-1-associated myelopathy/tropical spastic paraparesis (HAM/TSP). HTLV-1 Tax-expressing cells show resistance to apoptosis induced by Fas ligand (FasL) and tumor necrosis factor (TNF)-related apoptosis-inducing ligand (TRAIL). The regulation of Tax on the autophagy pathway in HeLa cells and peripheral T cells was recently reported, but the function and underlying molecular mechanism of the Tax-regulated autophagy are not yet well defined. Here, we report that HTLV-1 Tax deregulates the autophagy pathway, which plays a protective role during the death receptor (DR)-mediated apoptosis of human U251 astroglioma cells. The cellular FLICE-inhibitory protein (c-FLIP), which is upregulated by Tax, also contributes to the resistance against DR-mediated apoptosis. Both Tax-induced autophagy and Tax-induced c-FLIP expression require Tax-induced activation of IκB kinases (IKK). Furthermore, Tax-induced c-FLIP expression is regulated through the Tax-IKK-NF-κB signaling pathway, whereas Tax-triggered autophagy depends on the activation of IKK but not the activation of NF-κB. In addition, DR-mediated apoptosis is correlated with the degradation of Tax, which can be facilitated by the inhibitors of autophagy.

IMPORTANCE

Our study reveals that Tax-deregulated autophagy is a protective mechanism for DR-mediated apoptosis. The molecular mechanism of Tax-induced autophagy is also illuminated, which is different from Tax-increased c-FLIP. Tax can be degraded via manipulation of autophagy and TRAIL-induced apoptosis. These results outline a complex regulatory network between and among apoptosis, autophagy, and Tax and also present evidence that autophagy represents a new possible target for therapeutic intervention for the HTVL-1 related diseases.

Human T-cell leukemia virus type 1 (HTLV-1) is the etiologic agent of both adult T-cell leukemia/lymphoma (ATL) and HTLV-1-associated myelopathy/tropical spastic paraparesis (HAM/TSP) (1, 2). It has been demonstrated that the major characteristic of ATL is rapid proliferation and malignant transformation of HTLV-1-infected $CD4^+$ T cells in human peripheral blood (PB) (3). Unlike ATL, HAM/TSP is mainly associated with chronic and progressive inflammation of the central nervous system (CNS) (4). During the course of HAM/TSP, the intrusion of HTLV-1-infected lymphocytes from the PB into the CNS may lead to the production of proinflammatory cytokines/chemokines, which would ultimately result in neurodegeneration (4, 5). In addition, histological studies conducted in HAM/TSP patients suggest that HTLV-1-infected resident CNS cells, including astrocytes and oligodendrocytes, also contribute to the progression of HAM/TSP (6, 7). Astrocytes are the most abundant cells in the CNS and perform many functions, including maintaining the physical integrity of the blood-brain barrier (BBB), providing nutrients to neuronal cells, and mediating the extracellular ion balance in the CNS (8). A previous study has shown that the *in vitro* infection of human astrocytes with HTLV-1 results in the release of proinflammatory cytokines (9). Furthermore, it has been found that neuropilin-1 and glucose transporter protein 1 are involved in HTLV-1 infection of U87 astroglioma cells and human primary astrocytes (10). Overall, these available data suggest that HTLV-1-infected astrocytes might be involved in the progression of HAM/TSP.

The viral oncoprotein Tax, encoded by the HTLV-1 genome, is thought to play a crucial role in the progression that leads to HTLV-1-related diseases (3, 11). Tax causes the transformation of $CD4^+$ T cells through the activation of regulatory factors that are involved in T cell replication and interferes with DNA repair to ultimately increase genetic instability (12, 13). In addition, Tax protects HTLV-1-infected cells from cell cycle arrest and apoptosis and, thus, facilitates the escape of HTLV-1 from immune surveillance (14–16). The Tax-mediated activation of cyclic AMP (cAMP)-responsive element-binding protein (CREB), NF-κB, and serum responsive factor (SRF) is critical for the biological functions of Tax (17, 18). It has been reported that Tax-induced activation of NF-κB at multiple levels is required for T cell transformation. In the cytoplasm, Tax binds directly to IKKγ; this

Received 14 October 2013 **Accepted** 15 December 2013

Published ahead of print 18 December 2013

Editor: S. R. Ross

Address correspondence to Dexian Zheng, zhengdx@pumc.edu.cn, or Yanxin Liu, liuyx2000@yeah.net.

doi:10.1128/JVI.03025-13

binding triggers the constitutive phosphorylation and degradation of IκB, which enables the translocation of NF-κB to the nucleus. In the nucleus, Tax recruits RelA and other transcriptional components to form transcriptional hot spots increasing NF-κB activation. In addition, Tax is shown to induce the processing of p100 to yield p52 for the activation of the noncanonical NF-κB pathway (19, 20). The constitutive activation of NF-κB not only promotes the survival and transformation of HTLV-1-infected cells (21, 22) but also induces the resistance of these cells to many apoptosis inducers, including gamma irradiation, cisplatin, Fas ligand (FasL), and tumor necrosis factor (TNF)-related apoptosis-inducing ligand (TRAIL) (23–27).

TRAIL, a member of the structurally related TNF superfamily (28), induces apoptosis of a variety of tumor cells and virus-infected cells through the interaction with its two receptors, DR4/TRAIL-R1 and DR5/TRAIL-R2 (29). The binding of TRAIL to DR4 and DR5 induces trimerization of the receptors and the subsequent recruitment of procaspase-8 (FADD-like interleukin-1β-converting enzyme [FLICE]) or procaspase-10 through the adaptor protein Fas-associated death domain (FADD) to form the death-inducing signaling complex (DISC). The formation of DISC is followed by activation of caspase-3, which ultimately results in cell death via apoptosis. In some cells, Bid, a Bcl-2 protein family member, can be activated by caspase-8 or -10 to induce mitochondrion-mediated apoptosis (30, 31). One major regulator of the receptor-mediated apoptosis at the DISC level is the cellular FLICE-inhibitory protein (c-FLIP) (32). It has been reported that three splice variants of c-FLIP (c-FLIP$_L$, c-FLIP$_R$, and c-FLIP$_S$) can be detected at the protein level and that the expression of c-FLIP is regulated through multiple pathways, such as the MAP kinase, phosphatidylinositol 3-kinase (PI3K), and NF-κB pathways (33–35). It has been demonstrated that the expression of c-FLIP is increased in ATL cells and HTLV-1-infected Tax-expressing T cells and that this increase contributes to the resistance of these cells to FasL- and TRAIL-induced apoptosis (25, 26, 36).

Autophagy is a lysosomal degradation pathway that degrades long-lived proteins and cytoplasmic organelles into basic biomolecules to recycle energy and nutrients. During autophagy, parts of or entire organelles are sequestered into double-membrane autophagosomes, which subsequently fuse with lysosomes, where the sequestered contents undergo degradation (37, 38). In many cellular settings, the first regulatory step involves the inactivation of the mammalian target of rapamycin (mTOR), which leads to the activation of a set of autophagy-regulating genes (Atg genes) and the subsequent formation of autophagosomes (39). During autophagosome formation, a cytosolic form of LC3 (LC3-I) is conjugated to phosphatidylethanolamine (PE) to form an LC3-PE conjugate (LC3-II), which is then recruited to autophagosomal membranes. Thus, the conversion of LC3-I to LC3-II is commonly considered a characteristic marker of autophagy (40). The induction of autophagy is tightly regulated by diverse extracellular and intracellular signals, including nutrients, growth factors, intracellular ATP levels, and hypoxia (38). In addition, autophagy is implicated in the regulation of retrovirus-host interactions. It was shown in a recent report that HTLV-1 infection and Tax protein expression increase autophagosome accumulation by blocking the fusion of autophagosomes to lysosomes in HeLa cells and Jurkat T cells (41). In another interesting report, it was indicated that HTLV-2 Tax could also induce autophagy by interacting with the autophagy molecule complex containing Beclin1 and PI3K class III, and Tax2-mediated autophagy promoted survival and proliferation of the immortalized CD4$^+$ T cells (42).

Here, we found that HTLV-1 Tax protein increases autophagosome accumulation in human astroglioma cells, primary astrocytes, and Jurkat T cells as well. In addition, Tax-deregulated autophagy helps protect human astroglioma cells from TRAIL receptor-mediated apoptosis. We showed that Tax-induced upregulation of c-FLIP also contributes to the resistance to TRAIL-induced apoptosis. We further demonstrated that Tax-mediated c-FLIP expression requires both the phosphorylation of IKK and the transcriptional activation of NF-κB, but Tax-induced autophagy is dependent only on the activation of IKK. Finally, we showed that inhibition of Tax-deregulated autophagy promotes Tax degradation induced by TRAIL-mediated apoptosis.

MATERIALS AND METHODS

Cells, reagents, and antibodies. The human HEK293T, U251, and Jurkat E6-1 cell lines were obtained from the American Type Culture Collection (ATCC, Manassas, VA, USA). Normal human astrocytes (HA) from human brain tissue were purchased from ScienCell Research Laboratories (Carlsbad, CA, USA). The HEK293T and U251 cells were maintained in Dulbecco's modified Eagle medium (DMEM) (Gibco, Grand Island, NY, USA) supplemented with 10% fetal bovine serum (FBS). The Jurkat E6-1 cells were cultured in RPMI 1640 (Gibco) supplemented with 10% FBS. The normal human astrocytes were cultured in astrocyte medium (ScienCell, Carlsbad, CA, USA).

Recombinant soluble TRAIL (amino acids 95 to 281, nontagged) and the mouse anti-human DR5 monoclonal antibody AD5-10 (IgG3) were prepared as described by Guo et al. (43). Chloroquine, 3-MA, and MG-132 were purchased from Sigma (St. Louis, MO, USA). LY294002 was purchased from Merck Chemicals (Darmstadt, Germany). PS-341 was purchased from LC Laboratories (Woburn, MA, USA). The z-VAD-fmk inhibitor was purchased from R&D Systems (Minneapolis, MN, USA).

Antibodies against caspase-8, caspase-3, caspase-9, phospho-IKKα/β, IKKα, IKKβ, p65, phospho-mTOR, and phospho-AMPKα were purchased from Cell Signaling Technology (Beverly, MA, USA). Anti-LC3 was obtained from Sigma. Anti-BECN1 and anti-IκBα were purchased from Santa Cruz Biotechnology (Santa Cruz, CA, USA). Anti-IKKγ was obtained from the Proteintech Group (Chicago, IL, USA), and anti-Flag and anti-green fluorescent protein (GFP) were purchased from Abmart (Shanghai, China). Anti-c-FLIP was purchased from Alexis (Farmingdale, NY, USA), and horseradish peroxidase (HRP)-conjugated anti-GAPDH was obtained from KangChen Biotech (Shanghai, China).

Preparation of lentiviral vectors. All of the constructs for gene overexpression were derived from the pWPXL-EGFP lentiviral vector (Addgene plasmid 12257, carrying the enhanced-GFP [EGFP] gene). The DNA fragments corresponding to the coding sequences of wild-type Flag-tagged Tax, the Flag-tagged Tax M22 mutant (^{137}GL→AS), the Flag-tagged Tax M47 mutant (^{319}LL→RS), IκBα-DN (S32A/S36A), the GFP-LC3 fusion gene, and the disordered EGFP open reading frame (empty expression cassette) were amplified via PCR and subcloned into pWPXL-EGFP through replacement of the EGFP fragment. All the Flag tags are located on the C terminus of Tax and its mutants. These recombinant lentiviral vectors were cotransfected into HEK293T cells with pMD2.G and psPAX2 using VigoFect (Vigorous, Beijing, China). The supernatants were collected 3 days after transfection, centrifuged at 2,500 × *g* for 10 min, filtered through a 0.45-μm-pore-size filter, pooled, and subjected to ultrafiltration with a Centricon Plus-70 centrifugal filter device (Millipore, Billerica, MA, USA). The concentrated virus stocks were aliquoted and frozen at −80°C. Titers of virus were determined by infecting 293T cells with serially diluted virus stock in culture medium, and GFP expression in 293T cells after 72 h of infection was analyzed by flow cytometry. Astroglioma cells, primary astrocytes, and Jurkat T cells were infected with lentivirus (multiplicity of infection [MOI] = 3; in some experiments,

the MOI was 1) in complete medium for 12 h under normal culture conditions. The medium containing virus was removed, and then the cells were washed and cultured in fresh complete medium.

The short hairpin RNAs (shRNA) targeting c-FLIP, Beclin-1, IKKα, IKKβ, and p65 were cloned into pLL3.7 lentiviral vectors. The following targeting sequences were used: c-$FLIP_L$ and c-$FLIP_S$, 5′-GGA GCA GGG ACA AGT TAC A-3′; Beclin-1, 5′-GCT GGA GAT GTT CAG AAC A-3′; IKKα, 5′-GCA ATT AAG TCT TGT CGC C-3′; IKKβ, 5′-GGA GAT CCA GAT CAT GAG A-3′; and p65, 5′-GGA TTG AGG AGA AAC GTA A-3′. The lentiviral stocks were prepared through cotransfection of these recombinant pLL3.7 vectors and the pRSV-Rev, pMDLg/pRRE, and pMD2.G packaging vectors using the methods described above.

Real-time PCR. The U251 cells infected with the LVs were lysed, and total RNA was isolated with the TRIzol reagent (Invitrogen, Carlsbad, CA, USA). First-strand cDNA was synthesized using 4 μg of the total RNA with the M-MLV reverse transcriptase (Promega, Madison, WI, USA). The real-time PCR was performed using SYBR premixed *Ex Taq* II (TaKaRa, Dalian, China) in the Bio-Rad iQ5 detection system (Bio-Rad, Hercules, CA, USA) according to the manufacturer's instructions. The following gene-specific primer pairs for c-$FLIP_L$, c-$FLIP_S$, and GAPDH were employed: c-$FLIP_L$, 5′-CCT AGG AAT CTG CCT GAT AAT CGA-3′ and 5′-TGG GAT ATA CCA TGC ATA CTG AGA-3′; c-$FLIP_S$, 5′-GCA GCA ATC CAA AAG AGT CTC A-3′ and 5′-ATT TCC AAG AAT TTT CAG ATC AGG-3′; and GAPDH, 5′-CCG TCT AGA AAA ACC TGC C-3′ and 5′-AGC CAA ATT CGT TGT CAT ACC-3′.

Western blot analysis. After the specified treatments, the cells were harvested and lysed with radioimmunoprecipitation assay (RIPA) buffer (0.15 M NaCl, 1% NP-40, 0.01 M deoxycholate, 0.1% SDS, 0.05 M Tris-HCl [pH 8.0], 1 mM sodium orthovanadate, 1 mM phenylmethylsulfonyl fluoride, 10 μg/ml aprotinin, 10 μg/ml pepstatin, and 10 μg/ml leupeptin). The obtained protein concentrations were determined using the bicinchoninic acid (BCA) protein assay kit (Thermo Scientific, Rockford, IL, USA). A total of 40 μg protein was electrophoresed on an 8% (only for the p-mTOR analysis) or 12% SDS-PAGE gel and transferred to a polyvinylidene fluoride membrane (Amersham Biosciences, Buckinghamshire, United Kingdom). The membrane was blocked with 5% nonfat dry milk or bovine serum albumin (BSA) in Tris-buffered saline–Tween (TBS-T) buffer (20 mM Tris-HCl [pH 7.4], 8 g/liter NaCl and 0.1% Tween 20) for 1 h at room temperature and then incubated with the appropriate primary antibody in TBS-T buffer containing 5% nonfat dry milk or BSA at 4°C overnight. The membrane was next probed with the appropriate horseradish peroxidase (HRP)-conjugated secondary antibody at room temperature for 2 h, and the proteins were detected with the Immobilon Western HRP substrate (Millipore).

Cell viability assay. U251 cells infected with the appropriate lentiviral vectors were plated in 96-well plates at a density of 1×10^4 cells per well, pretreated with various inhibitors for 3 h, and then treated with various concentrations of TRAIL or AD5-10 for 12 h. Cell viability was determined using the CellTiter 96 AQ_{ueous} nonradioactive cell proliferation assay (MTS assay) according to the manufacturer's instructions (Promega, Madison, WI, USA).

Apoptosis analysis. For nuclear staining, the cells were fixed for 20 min in 4% paraformaldehyde in phosphate-buffered saline (PBS) and then stained with 1 μg/ml Hoechst 33258 in PBS for 15 min. Apoptosis was visualized using fluorescence microscopy. For Annexin V/7-AAD staining, cells subjected to the appropriate treatments for various times were stained using the Annexin V-PE kit according to the manufacturer's instructions (BD Biosciences, Franklin Lakes, NJ, USA). The samples were then analyzed with a flow cytometer (FACScan, Becton, Dickinson, Germany).

Fluorescence and confocal laser-scanning microscopy. Cells were first infected with lentivirus (LV) encoding GFP-LC3, and after 4 days, the percentages of GFP-positive cells were examined via flow cytometer. Almost all of the cells (>95%) were GFP positive. Then, cells expressing GFP-LC3 were infected with LV-Empty or LV-Tax. To analyze the percentage of cells that exhibited cytoplasmic GFP-LC3 aggregations in each group, images were acquired through fluorescence microscopy, and the total cell numbers and the number of autophagic cells containing GFP-LC3 fluorescent dots were counted. Approximately 350 cells were analyzed in each group. To determine the number of GFP-LC3 dots (autophagic vacuoles) per cell, the LV-infected cells were grown on glass coverslips in 6-well plates. After the specified treatments, the cells were washed twice with PBS and fixed with 4% paraformaldehyde in PBS for 20 min. Nuclear counterstaining was performed with Hoechst 33258 as described above. The coverslips were mounted on slides using ProLong antifade solution and examined with a Zeiss LSM 510 META laser-scanning confocal microscope (Carl Zeiss, Jena, Germany).

Transmission electron microscopy. U251 cells were seeded into 6-well plates. Four days after LV infection, the cells were washed twice with 0.1 M phosphate buffer and harvested via centrifugation at $150 \times g$ for 10 min. The cells were fixed with 2.5% glutaraldehyde in 0.1 M phosphate buffer at 4°C for 30 min, then fixed again in 1% OsO_4 for 1 h, dehydrated using increasing concentrations of acetone, and gradually infiltrated with epoxy resin. Ultrathin sections were obtained and stained with uranyl acetate and lead citrate. Electron micrographs of the sections were obtained with a JEM-1010 transmission electron microscope (JEOL, Tokyo, Japan).

Statistical analysis. All data are presented as the means ± standard errors from three independent experiments. The data were analyzed using Microsoft Excel (Microsoft, Redmond, WA, USA), and the statistical significance of the differences was evaluated using Student's *t* test. Differences with probability values below 0.05 ($P < 0.05$) were considered significant, and differences with probability values below 0.01 ($P < 0.01$) were considered highly significant.

RESULTS

HTLV-1 Tax increases autophagosomes accumulation. The effect of HTLV-1 Tax on apoptosis has been widely studied. Recently, the regulation by Tax of the autophagy pathway was also reported (41, 42). However, the relationship between Tax-regulated apoptosis and autophagy is still unclear. In the present study, HTLV-1 Tax was introduced into TRAIL-sensitive U251 astroglioma cells to establish a model system that could be used to investigate the effect of Tax on autophagy and death receptor-mediated apoptosis. The U251 cells were infected with a lentivirus (LV) encoding EGFP (control) or HTLV-1 Tax-Flag. The efficiency of LV-EGFP infection was determined by determining the numbers of EGFP-positive cells via flow cytometry 4 days postinfection, which demonstrated that more than 93% of the cells expressed EGFP encoded by lentivirus. The expression of the HTLV-1 Tax-Flag protein was also confirmed by Western blotting. The level of LC3-II protein, which is a marker of the autophagosome membrane, was found to be significantly increased in the LV-Tax-infected U251 cells compared with LV-EGFP-infected cells after 4 days of infection (Fig. 1A). The intracellular localization of GFP-LC3 corroborated the presence of GFP-LC3 aggregates as cytoplasmic dots in the U251 cells transfected with LV-Tax (Fig. 1B), and the quantitative assay demonstrated a higher percentage of cells with GFP-LC3 dots in Tax-expressing cells than in the empty vector control. Accordingly, an increase in the number of autophagosome was also observed in the Tax-expressing U251 cells via transmission electron microscopy (Fig. 1C).

Previous studies have shown that the astrocytes of HAM/TSP patients might be infected by HTLV-1 (6, 7). To determine whether HTLV-1 Tax induces autophagy in primary astrocytes, normal human astrocytes were infected with the above-mentioned LVs. As shown in Fig. 1D, expression of the Tax protein

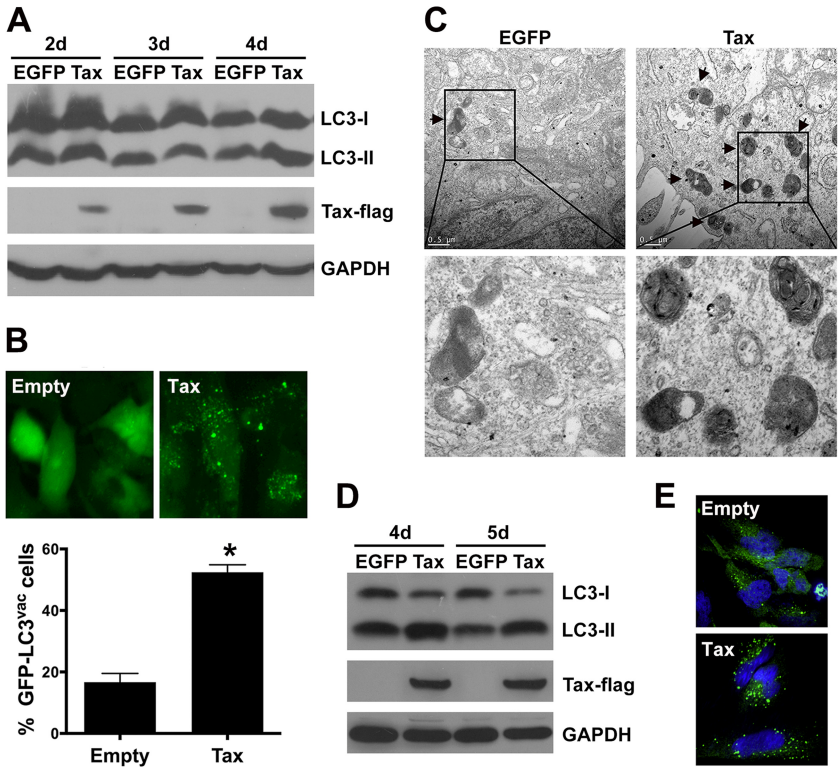

FIG 1 HTLV-1 Tax increases autophagosome accumulation. (A) Detection of LC3-I and LC3-II expression. U251 cells (2×10^5 cells) were infected with LV-EGFP or LV-Tax for 2 to 4 days. Forty micrograms total protein was loaded onto SDS-PAGE gels and further analyzed by Western blotting to detect the conversion of LC3-I to LC3-II and Tax expression. (B) GFP-LC3 aggregation was visualized via fluorescence microscopy. U251 cells expressing GFP-LC3 were infected with LV-Empty (empty expression cassette) or LV-Tax; after 4 days, the GFP-LC3 aggregations in the cells were assessed via fluorescence microscopy. Representative images are shown (top), and the percentage of cells with GFP-LC3 puncta (% GFP-$LC3^{vac}$ cells) is presented (bottom; values are means and standard deviations [SD]; *, $P < 0.01$). (C) Autophagic vacuoles were detected via transmission electron microscopy. U251 cells expressing EGFP or Tax were processed 4 days after lentiviral infection for transmission electron microscopy. Representative images are shown, and the arrows indicate autophagic vacuoles. Bars, 0.5 μm. (D and E) Tax induces autophagosome accumulation in primary human astrocytoma cells. Astrocytes (5×10^5) were infected with LV-EGFP or LV-Tax (MOI = 3), and after 4 and 5 days of infection, 40 μg total protein was used in Western blot assays to detect the conversion of LC3-I to LC3-II (D). GFP-LC3 dots were analyzed using confocal microscopy 4 days after infection. Astrocytes expressing GFP-LC3 were infected with LV-Empty or LV-Tax. The GFP-LC3 aggregations were assessed via confocal microscopy after 4 days of infection. Cell nuclei were stained with Hoechst 33258. Representative images are shown (E).

resulted in extensive conversion of LC3-I to LC3-II compared with the EGFP-expressing control cells after 4 to 5 days of LV infection. Meanwhile, the number of GFP-LC3 dots was increased in Tax-expressing astrocytes (Fig. 1E). Furthermore, Tax-induced conversion of LC3-I to LC3-II was also observed in Jurkat T lymphocytes and 293T cells (data not shown). These data indicate that HTLV-1 Tax deregulates the autophagy pathway, resulting in increased autophagosome accumulation.

Tax expression inhibits death receptor-mediated apoptosis. It was reported previously that HTLV-1 infection led to resistance to TRAIL-induced apoptosis in human T cells (36). To further study whether the Tax protein could manipulate death receptor-mediated apoptotic signaling in U251 cells, the cells were infected with LV-EGFP or LV-Tax and then treated with various concentrations of recombinant soluble TRAIL or AD5-10 (an agonistic anti-DR5 antibody) (43) for 12 h. Cell viability was determined through an MTS assay. As shown in Fig. 2A, the viability of Tax-expressing U251 cells treated with TRAIL or AD5-10 was much higher than that of EGFP-expressing counterparts. Meanwhile, Tax expression did not affect the growth rate of U251 cells (data not shown). To further determine the apoptosis inhibition mediated by Tax, EGFP- or Tax-expressing U251 cells treated with TRAIL were stained with Hoechst 33258 to visualize chromosome condensation via fluorescence microscopy (Fig. 2B) or stained with Annexin V-PE to identify the externalization of phosphatidylserine at an earlier stage of apoptosis (Fig. 2C). The data indicated that TRAIL treatment induced an obvious chromosome condensation in the EGFP-expressing cells but not in the Tax-expressing cells (Fig. 2B). Annexin V staining confirmed that TRAIL induced more apoptosis in the EGFP-expressing cells than in Tax-expressing cells (Fig. 2C). TRAIL or AD5-10 stimulation usually activates a caspase cascade, leading to apoptosis. To confirm the impact of Tax expression on TRAIL-induced caspase activation, the cell lysates from Tax-expressing U251 cells treated with recombinant soluble TRAIL or AD5-10 were further analyzed via Western blotting assay. The results showed that Tax expression markedly suppressed the activation of caspase-8, caspase-3, and caspase-9 in U251 cells treated with TRAIL or AD5-10 (Fig. 2D), indicating that Tax expression indeed inhibits the death receptor-mediated apoptosis of human astroglioma cells.

Inhibition of autophagy potentiates death receptor-mediated apoptosis. Autophagy is considered to be a prosurvival re-

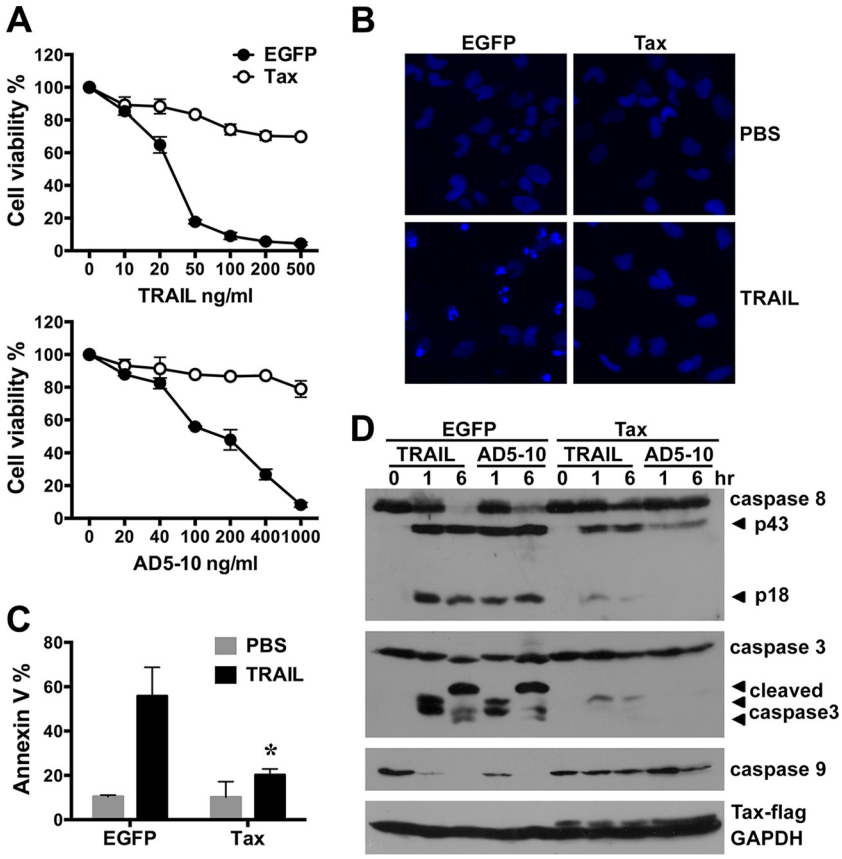

FIG 2 Tax suppresses TRAIL-induced apoptosis in U251 astroglioma cells. U251 cells were infected with LV-EGFP or LV-Tax (MOI = 3) for 4 days and then treated with recombinant soluble TRAIL or the anti-DR5 agonistic monoclonal antibody AD5-10 at the indicated concentrations for 0 to 12 h. (A) The cell viability after TRAIL or AD5-10 treatment for 12 h was determined using MTS assays (mean ± SD; $n = 3$). (B and C) Apoptosis in cells treated with 50 ng/ml TRAIL or PBS (control) for 6 h was detected through fluorescence microscopy analysis of Hoechst 33258-stained cells (B) and flow cytometry analysis of PE-conjugated Annexin V-stained cells (C). The mean percentages of Annexin V-positive cells from three independent experiments are shown (mean ± SD; *, $P < 0.01$ compared with TRAIL-treated EGFP-expressing cells). (D) The activation of caspase-8, -3, and -9 in EGFP- and Tax-expressing cells treated with PBS, 50 ng/ml TRAIL, or 100 ng/ml AD5-10 for 1 and 6 h was analyzed by Western blotting. GAPDH was used as a protein loading control.

sponse that protects cells against stress or nutrient starvation and a cell protection mechanism against apoptosis induced by chemotherapeutic agents and recombinant soluble TRAIL (44–47). To further investigate whether the induction of autophagy in Tax-expressing cells might be a defense mechanism to prevent death receptor-mediated apoptosis, Tax-expressing U251 cells were treated with the autophagy inhibitors 3-MA and LY294002, which are PI3 kinase inhibitors that prevent autophagy at an early stage, or chloroquine, which inhibits the fusion of the autophagosome with the lysosome and, thus, suppresses autophagy at a later stage (48). As shown in Fig. 3A and B, these inhibitors alone had negligible effects on cell viability; however, pretreatment with 3-MA, LY294002, or chloroquine significantly increased TRAIL-induced cell death in Tax-expressing U251 cells. In addition, AD5-10-induced cell death was also potentiated by 3-MA treatment (data not shown). The effect of 3-MA on apoptotic signaling was further confirmed by Western blotting assay. As shown in Fig. 3C, 3-MA alone inhibited the Tax-induced accumulation of LC3-II. In addition, 3-MA and TRAIL increased the activation of caspase-8 and caspase-3 in Tax-expressing U251 cells. These data suggest that the pharmacological inhibition of autophagy increases the sensitivity of Tax-expressing U251 cells to TRAIL treatment. Interestingly, the protein expression level of Tax was markedly decreased in the cells treated with combination of 3-MA and TRAIL, suggesting that Tax degradation might be regulated by TRAIL and autophagy signaling.

Because pharmacological inhibitors of autophagy might have undesired side effects, an shRNA specifically targeting Beclin-1 (shBECN1) was used to inhibit the autophagy pathway in the experimental system (49, 50). As shown in Fig. 3D, knockdown of Beclin-1 expression by shBECN1 suppressed the accumulation of LC3-II. Compared with the control cells, the viability of Tax-expressing cells transfected with shBECN1 decreased after treatment with TRAIL (Fig. 3D). Collectively, these data demonstrate that inhibition of autophagy pathway promotes the TRAIL-induced apoptosis of Tax-expressing U251 cells.

Tax-induced c-FLIP expression also contributes to the resistance against death receptor-mediated apoptosis. It has previously been reported that c-FLIP expression is upregulated in HTLV-1-infected and HTLV-1 Tax-expressing T cells and that the expression of this protein plays an important role in the resistance of the cells against FasL- or TRAIL-induced apoptosis (25, 26, 36). We therefore investigated the expression of c-FLIP in Tax-expressing U251 cells. Real-time quantitative PCR revealed that the

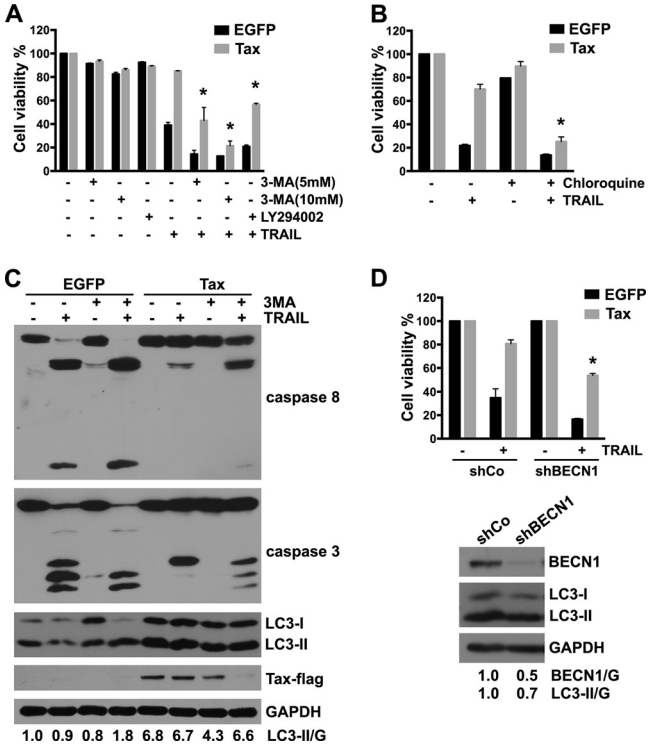

FIG 3 Inhibition of autophagy pathway sensitizes Tax-expressing U251 cells to TRAIL-induced apoptosis. (A and B) U251 cells were infected with LV-EGFP or LV-Tax for 4 days, pretreated with 3-MA (5 mM or 10 mM), LY294002 (20 μM) (A), or 100 μM chloroquine (B) for 3 h, and then cultured for 12 h in the presence or absence of 50 ng/ml TRAIL. Cell viability was determined using MTS assays (mean ± SD; $n = 3$; *, $P < 0.01$ compared with TRAIL-treated Tax-expressing cells). (C) U251 cells were infected as for panels A and B, pretreated with 10 mM 3-MA for 3 h, and then treated with 50 ng/ml TRAIL for 6 h. The cell lysates were analyzed via Western blotting to determine the expression of c-FLIP, LC3, and Tax and the activation of caspase-8 and caspase-3. GAPDH was used as a protein loading control. Protein quantification was performed via densitometry, and the ratios of LC3-II to GAPDH are shown under the respective blots. (D) U251 cells were infected with LV-EGFP or LV-Tax for 12 h and then with LVs encoding Beclin-1 shRNA (shBECN1) or no shRNA (shCo) for another 12 h (MOI = 3). After 4 days, the cells were treated with 50 ng/ml TRAIL or PBS (control) for 12 h. Cell viability was determined via MTS assays (mean ± SD; $n = 3$; *, $P < 0.01$ compared with TRAIL-treated cells expressing Tax and shCo). The efficacies of BECN1 knockdown and LC3 expression are shown in the bottom panel. U251 cells were infected with LV-shCo or LV-shBECN1 for 4 days. The cell lysates were analyzed by Western blotting to determine the expression of BECN1 and LC3.

levels of c-FLIP$_L$ mRNA in cells infected with LV-Tax increased 3.1- and 3.8-fold at 48 h and 72 h postinfection, respectively, while those of c-FLIP$_S$ mRNA increased 4.0- and 4.7-fold, respectively (Fig. 4A). The levels of c-FLIP$_L$ and c-FLIP$_S$ protein were further determined by Western blot analysis. As shown in Fig. 4B, c-FLIP$_L$ and c-FLIP$_S$ were upregulated in the Tax-expressing cells, and the difference in c-FLIP$_S$ protein expression was greater than the difference in c-FLIP$_L$ expression. Consistent with what was observed in U251 cells, the increased expression of c-FLIP$_L$ and c-FLIP$_S$ was also observed in Tax-expressing primary human astrocytes (Fig. 4C) and Jurkat T lymphocytes (data not shown).

To further analyze the relationship between increased c-FLIP levels and the resistance to TRAIL-induced apoptosis, U251 cells were infected first with LV-EGFP or LV-Tax and then with a lentivirus encoding a c-FLIP-specific shRNA (shFLIP) or control shRNA (shCo) and subsequently treated with TRAIL. Western blotting assays showed that in Tax-expressing c-FLIP knockdown cells, the TRAIL treatment increased the amount of cleaved p43-FLIP, which is a 43-kDa cleavage product of c-FLIP and generated from c-FLIP$_L$ at the DISC as a result of procaspase-8 cleavage at D376 (51, 52), and the active subunits of caspase-8 and -3 (Fig. 4D); meanwhile, c-FLIP knockdown obviously decreased the cell viability of Tax-expressing cells treated with TRAIL (Fig. 4E), indicating that downregulation of c-FLIP could partially overcome the TRAIL resistance induced by Tax. In addition, we found that inhibition of autophagy by 3-MA could further promote TRAIL-induced reduction of cell viability in c-FLIP-downregulated Tax-expressing cells (Fig. 4F).

Taken together, these data indicate that both c-FLIP upregulation and increased autophagy induced by HTLV-1 Tax contribute to the resistance against TRAIL-induced apoptosis.

Tax-induced c-FLIP expression and autophagy are correlated with the ability of Tax to activate IKK. Tax triggers gene transcription through NF-κB and CREB pathway (26, 53, 54). Recent reports have shown that Tax-induced c-FLIP expression in T cells requires the activation of NF-κB (26). To further examine the molecular mechanism underlying Tax-induced autophagy, the Tax mutants M22 and M47 were used in our study. The M22 mutant is defective for NF-κB activation but retains the ability to transactivate CREB-driven transcription. Conversely, the M47 mutant is defective for CREB activation but retains the ability to activate NF-κB (55). The effects of Tax, M22, and M47 on c-FLIP expression, NF-κB activation, and autophagy in U251 cells were subsequently analyzed. Significantly increased c-FLIP expression, IκBα degradation, and LC3-II accumulation were observed in Tax-expressing U251 cells and M47-expressing cells but not in M22-expressing cells (Fig. 5A). Transmission electron microscopy confirmed the presence of an increased number of autophagosomes in the Tax- and M47-expressing U251 cells compared with the M22- and EGFP-expressing cells (Fig. 5B). Increased GFP-LC3 aggregation (green dots) in the cytoplasm was also observed in the Tax- and M47-expressing cells via confocal microscopy (Fig. 5C). These data indicate that the Tax mutant M22, which is defective in IKK activation, is unable to stimulate autophagy and c-FLIP expression in U251 cells.

Next, we assessed the effects of the Tax mutants on the TRAIL-induced apoptosis of U251 cells. The activation of caspases was determined through an immunoblotting assay. Compared with what was observed in the EGFP-expressing cells, the expression of Tax or M47 inhibited the TRAIL-induced activation of caspase-8, -3, and -9, whereas the expression of M22 failed to affect the activation of these caspases (Fig. 5D). Accordingly, cell viability assays showed that apoptosis induced by TRAIL or the anti-DR5 agonistic monoclonal antibody AD5-10 was strongly suppressed in the Tax- and M47-expressing cells but not in the M22- and EGFP-expressing cells (Fig. 5E). These results demonstrate that the ability of Tax to activate IKK/NF-κB is essential for Tax-induced c-FLIP expression and autophagy, both of which play critical roles in the Tax-induced resistance to TRAIL.

Transcriptional activation of NF-κB is essential for Tax-induced c-FLIP expression but not Tax-induced autophagy. It has been reported that Tax-induced c-FLIP expression in human T cells involves activation of the IKK complex, degradation of IκBα, and the eventual transcriptional activation of NF-κB (26). To investigate whether these components in the NF-κB signaling path-

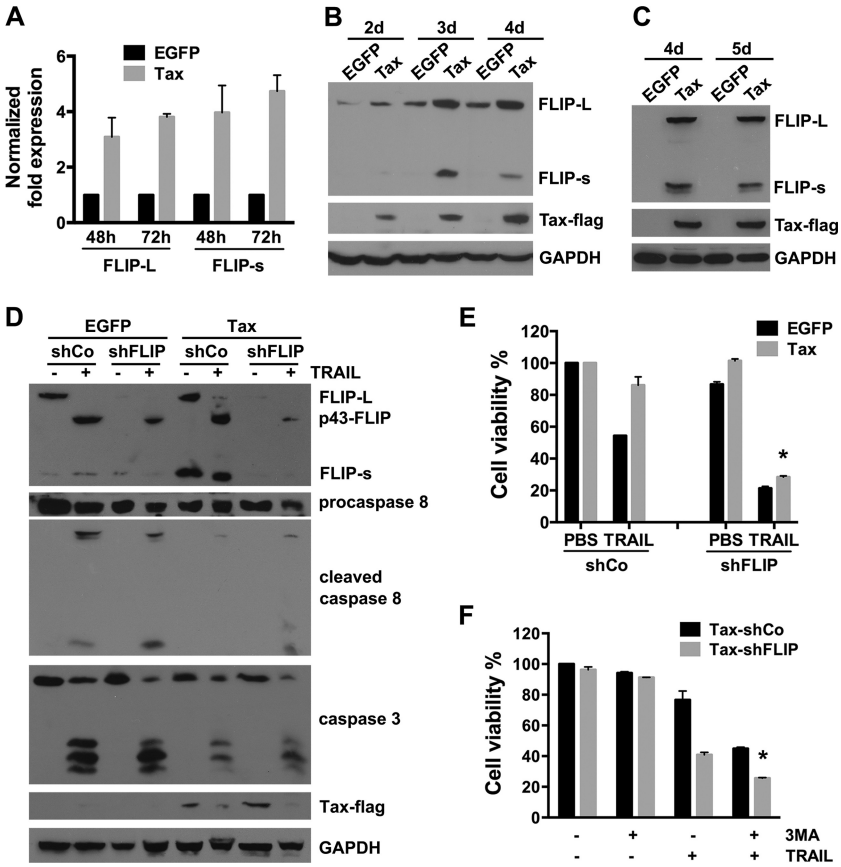

FIG 4 Tax-induced c-FLIP expression also protects U251 cells from TRAIL-induced apoptosis. (A) The expression of c-FLIP$_L$ and c-FLIP$_S$ mRNA in U251 cells infected with LV-EGFP or LV-Tax for the indicated times was assessed via real-time quantitative PCR. Data are presented as fold change in gene expression relative to EGFP-expressing cells (mean ± SD; $n = 3$). (B) Tax upregulates the level of c-FLIP protein expression. Western blot analysis of c-FLIP$_L$, c-FLIP$_S$, and Tax expression in U251 cells infected with the LVs for 2 to 4 days was carried out. GAPDH expression was used as a loading control. (C) Primary human astrocytoma cells were infected with LV-EGFP or LV-Tax (MOI = 3), and then the cell lysates of the primary human astrocytoma cells were analyzed 4 and 5 days after infection by Western blotting to detect the expressions of the c-FLIP and Tax-Flag proteins. (D and E) U251 cells were infected with LV-EGFP or LV-Tax for 24 h and then with LVs encoding c-FLIP shRNA (shFLIP) or no shRNA (shCo) (MOI = 3) for 3 days, after which they were treated with 50 ng/ml TRAIL for 6 h (D) or 12 h (E). The expression of c-FLIP and Tax and the activation of caspase-8 and caspase-3 were analyzed by Western blotting. The bands of procaspase-8 and cleaved caspase-8 were cut from two films with different exposure times. GAPDH was used as a loading control (D). Cell viability was detected via MTS assays (E) (mean ± SD; $n = 3$; *, $P < 0.01$ compared with TRAIL-treated cells expressing Tax and shCo). (F) Tax-expressing U251 cells were infected with LV-shFLIP or LV-shCo (MOI = 1) for 3 days, pretreated with 3-MA (10 mM) for 3 h, and then cultured for 12 h in the presence or absence of 20 ng/ml TRAIL. Cell viability was determined using MTS assays (mean ± SD; $n = 3$; *, $P < 0.01$ compared with TRAIL-only-treated Tax-shFLIP cells).

way are involved in Tax-induced autophagy, the effects of knockdown of IKKα, IKKβ, and p65 as well as overexpression of an IκBα dominant negative mutant (IκB-DN) on Tax-induced autophagy were examined in Tax-expressing U251 cells. As shown in Fig. 6A to C, downregulation of IKKα or IKKβ using shRNA not only inhibited Tax-induced c-FLIP expression but also suppressed the accumulation of LC3-II. However, knockdown of the p65 subunit of NF-κB or overexpression of IκB-DN only inhibited Tax-induced c-FLIP expression and failed to suppress LC3-II accumulation. These data indicate that the activation of NF-κB is necessary for Tax-induced c-FLIP expression but not for Tax-induced autophagy, which was mainly dependent upon IKK activation. Furthermore, analysis of whether the inhibition of IKK or NF-κB activation could facilitate the TRAIL-induced apoptosis of Tax-expressing U251 cells showed that the resistance of the cells to TRAIL-induced apoptosis could be partially reversed via downregulation of IKKα/β or p65 or overexpression of IκB-DN (Fig. 6D and E). These results confirm that all of these components (IKKα/β, IκBα, and p65) of the NF-κB signaling pathway contribute to the Tax-induced resistance of U251 cells to TRAIL-induced apoptosis.

Starvation-induced autophagy requires the activation of AMP-activated kinase (AMPK) and the inhibition of mTOR (39, 56). Criollo et al. reported that IKK-stimulated autophagy was controlled by the AMPK/mTOR pathway (57). Accordingly, we further observed that Tax expression in U251 cells induced the phosphorylation of IKKα/β and AMPKα and inhibited the phosphorylation of mTOR (Fig. 6F), suggesting that the IKK-AMPKα-mTOR signaling pathway may be involved in Tax-induced autophagy.

Enhancement of TRAIL-induced apoptosis promotes Tax degradation. We have so far observed that TRAIL induces Tax degradation in 3-MA-pretreated and c-FLIP-downregulated Tax-expressing U251 cells (Fig. 3C and 4D). In addition, the TRAIL-induced degradation of M22, but not Tax or M47, was observed (Fig. 5D). These data imply that although Tax-expressing U251

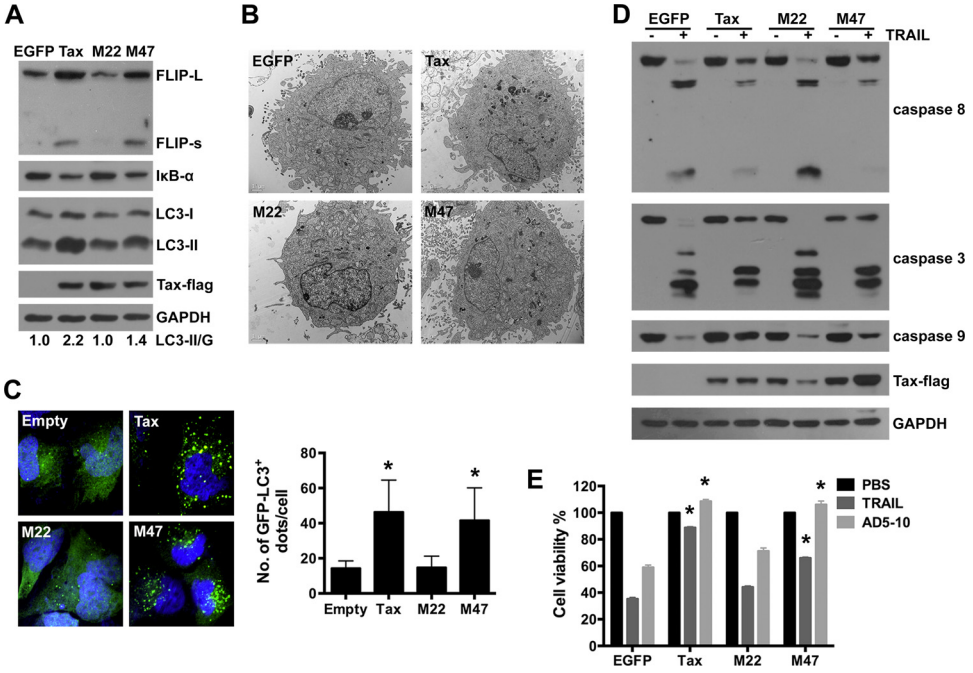

FIG 5 The Tax mutant M22 is unable to induce c-FLIP expression and autophagosome accumulation. (A) M22 has no effect on c-FLIP and LC3-II expression. U251 cells were infected with the indicated LVs; 4 days after the infection, the levels of c-FLIP$_L$, c-FLIP$_S$, and LC3 expression were analyzed by Western blotting. Protein quantification was performed via densitometry, and the ratios of LC3-II to GAPDH are shown under the respective blots. (B) U251 cells were infected as for panel A and processed for the detection of autophagic vacuoles through transmission electron microscopy. Representative images are shown (scale bars, 0.5 μm). (C) U251 cells expressing GFP-LC3 were infected with LV-Empty, Tax, M22, or M47 and analyzed using confocal microscopy 4 days after infection. Cell nuclei were stained with Hoechst 33258. Representative images are shown (left), and the number of GFP-LC3 dots per cell is reported (right) (mean ± SD; 20 cells; *, $P < 0.01$ compared with LV-Empty-infected cells). (D and E) M22 is unable to induce resistance to TRAIL-induced apoptosis. U251 cells were infected with the indicated LVs for 4 days and then treated with 50 ng/ml TRAIL for 6 h. The lysates were analyzed by Western blotting to assess caspase activation and the expression of Tax-Flag, M22-Flag, and M47-Flag (D). Alternatively, LV-infected U251 cells were treated with 50 ng/ml TRAIL or the anti-DR5 agonistic monoclonal antibody AD5-10 (100 ng/ml) for 12 h, after which cell viability was determined via MTS assays (mean ± SD; $n = 3$; *, $P < 0.01$ compared with TRAIL- or AD5-10-treated EGFP-expressing cells) (E).

cells are resistant to TRAIL-induced apoptosis, enhancement of TRAIL signaling through c-FLIP knockdown or autophagy suppression can promote Tax degradation. It has been reported that Tax binds directly to the IKK regulatory subunit IKKγ and stimulates the activity of the catalytic subunits IKKα and IKKβ (17, 58). Therefore, we further investigated whether these IKK subunits could be degraded as a result of Tax degradation induced by TRAIL and autophagy inhibition. As shown in Fig. 7A, the expression of IKKα and IκBα decreased, while the expression of IKKβ and IKKγ was rarely affected in EGFP-expressing U251 cells treated with TRAIL in the presence or absence of 3-MA. In Tax-expressing cells, TRAIL alone induced significant degradation of IKKβ but only a small amount of degradation of IKKα and Tax. Combination of 3-MA and TRAIL enhanced the TRAIL-induced degradation of IKKα, IKKβ, and Tax and meanwhile induced the activation of caspase-3; however, IKKγ was not affected by TRAIL alone or the combination of TRAIL and 3-MA (Fig. 7B). These results suggest that the TRAIL-induced degradation of activated IKKα/β and Tax can be promoted by autophagy inhibition. To explore the mechanism underlying the Tax degradation induced by TRAIL and 3-MA, the proteasome inhibitors MG132 and PS-341, the pan-caspase inhibitor z-VAD-fmk, and the endosomal acidification inhibitor chloroquine, which inhibits lysosomal protein degradation, were added to the experimental system. As shown in Fig. 7C, all of the inhibitors with the exception of the pan-caspase inhibitor z-VAD-fmk failed to inhibit the Tax degradation induced by the combination of TRAIL and 3-MA. More importantly, MG132, PS-341, and chloroquine promoted TRAIL-induced Tax degradation that was similar to that induced by 3-MA. Thus, TRAIL and 3-MA-induced Tax degradation is dependent on the activation of caspases; i.e., TRAIL-induced apoptosis promotes Tax degradation.

On the basis of these results, we propose that HTLV-1 Tax induces resistance to TRAIL-induced apoptosis, which is contributed to by the Tax-deregulated autophagy pathway and c-FLIP expression (Fig. 7D). Tax-induced c-FLIP expression is through the IKK-IκBα-NF-κB pathway, whereas Tax-increased autophagy requires IKK activation but not NF-κB activation (Fig. 7D). Additionally, enhancement of TRAIL-induced apoptosis signaling can promote the degradation of Tax, which is regulated by caspase activation (Fig. 7D).

DISCUSSION

Increasing evidence implies that virus infection-induced autophagy plays a role in the development of virus-related disease (59). It has been shown that autophagy is activated in mammalian cells by a variety of viruses, including human immunodeficiency virus (HIV), varicella-zoster virus, and influenza virus H9N2/G1 (60–62). HTLV-1 and HTLV-2 were recently reported to regulate autophagy pathway in Jurkat and CD4$^+$ T cells, respectively; how-

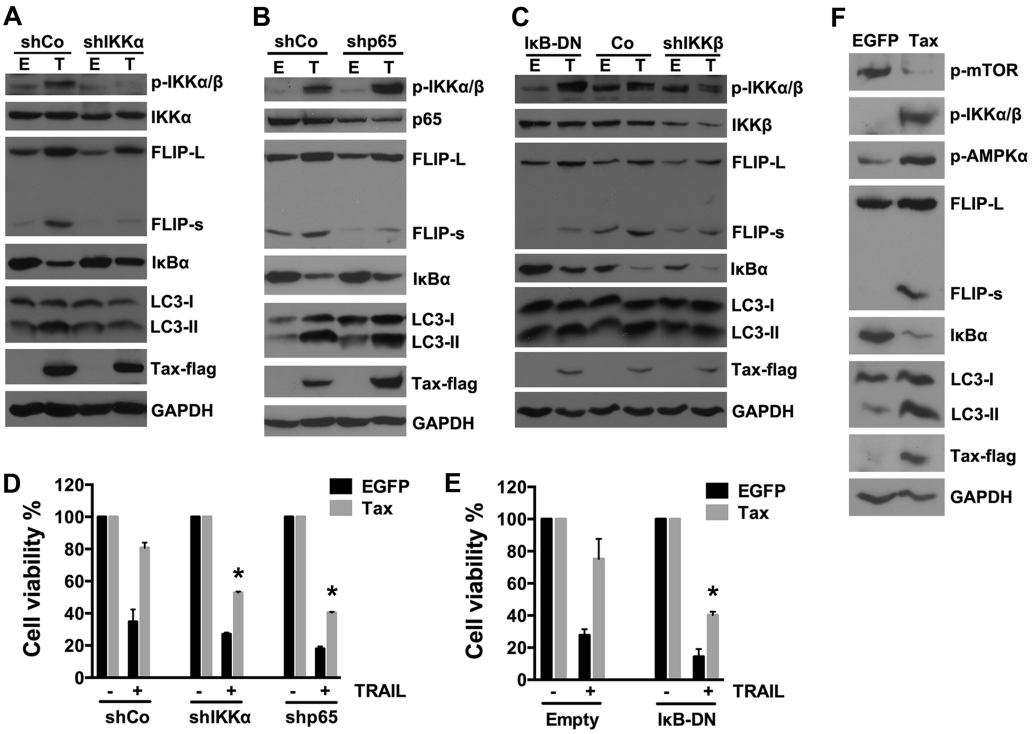

FIG 6 Activation of NF-κB is necessary for Tax-induced c-FLIP expression but not for Tax-increased autophagosome accumulation. (A to C) U251 cells were infected with LVs encoding no shRNA sequence (shCo), an shRNA targeting IKKα (A), IKKβ (C), or p65 (B), or IκB-DN mutant genes (C) for 3 days and then infected with LV-EGFP or LV-Tax. The knockdown efficacy, IκBα degradation, and c-FLIP and LC3-II expression levels were analyzed by Western blotting. (D and E) IKKα (D), p65 (D), and IκBα (E) contribute to Tax-induced TRAIL resistance. After the infection of the cells with LVs as described for panels A to C, the U251 cells were cultured in the presence or absence of 50 ng/ml TRAIL for 12 h. Cell viability was then determined via MTS assays (mean ± SD; $n = 3$; *, $P < 0.01$ compared with TRAIL-treated cells expressing Tax and shCo [D] or Tax and Empty [E]). (F) AMPKα and mTOR are involved in Tax-increased autophagosome accumulation. U251 cells were infected with LVs; 4 days after infection, the cell lysates were analyzed by Western blotting to determine IKK and AMPKα activation, mTOR inhibition, and c-FLIP and LC3-II expression levels.

ever, the biological significance of Tax-induced autophagy is still rarely known. Tang et al. reported that HTLV-1 Tax increased autophagy could enhance HTLV-1 replication and production by preventing the degradation of Tax (41). Another report showed that HTLV-2 Tax-mediated autophagy promoted survival and proliferation of immortalized T cells (42). In the present study, we have demonstrated that the HTLV-1 Tax protein induces autophagy, resulting in autophagosome accumulation in U251 cells, human primary astrocytes, and Jurkat T lymphocytes. Inhibition of autophagy pathway attenuates the TRAIL resistance induced by HTLV-1 Tax, suggesting that Tax induces resistance against TRAIL-induced apoptosis by deregulating autophagy as a protective mechanism.

Tax is responsible for the resistance against TRAIL- or FasL-induced apoptosis observed in HTLV-1-infected T cells (25, 26, 36). The Tax-induced expression of anti-apoptosis proteins, including Bcl-X_L and c-IAP2, has been observed in T cells; however, none of these proteins are able to inhibit FasL- or TRAIL-mediated apoptosis at the DISC level (26, 63). Here we observed that the TRAIL-induced activation of caspase-8 is inhibited in Tax-expressing U251 cells, and Okamoto et al. showed that Tax inhibits FasL-induced apoptosis at the DISC level (26). We further demonstrate that the Tax-induced increase of c-FLIP expression contributes to the resistance of cells to TRAIL and downregulation of c-FLIP can restore the sensitivity of Tax-expressing U251 cells to TRAIL. Tax-induced c-FLIP upregulation is considered a critical mechanism of the resistance to FasL in previous studies (25, 26). In addition, rocaglamide is reported to sensitize HTLV-1-infected T cells to FasL- and TRAIL-induced apoptosis through the translational suppression of c-FLIP expression (36). Accordingly, we observed that knockdown of c-FLIP almost entirely restored the sensitivity of Tax-expressing U251 cells to TRAIL (Fig. 4D), providing further evidence for the idea that c-FLIP plays an important role in Tax-induced TRAIL resistance.

In addition to the Tax-induced c-FLIP expression, the autophagy pathway deregulation by Tax was revealed as another mechanism of Tax-mediated TRAIL resistance in our study. The relationship between autophagy and apoptosis is a complicated issue that is still debated. Increasing amounts of accumulated data demonstrate that autophagy and apoptosis can be triggered by common upstream signals and that inhibition of autophagy can enhance apoptosis under particular conditions (48, 50). Certain chemotherapeutics, including temozolomide, resveratrol, and the phytochemical sulforaphane, are reported to induce both autophagy and apoptosis in tumor cells, and inhibition of autophagy could potentiate the apoptosis induced by these compounds (64–66). Besides its ability to induce apoptosis, TRAIL can induce autophagic cell death and a protective autophagic response (67, 68). The inhibition of autophagy through knockdown of Beclin-1 can enhance the sensitivity of TRAIL-resistant tumor cells to TRAIL (47). Han et al. demonstrated that inhibition of TRAIL-induced autophagy with Be-

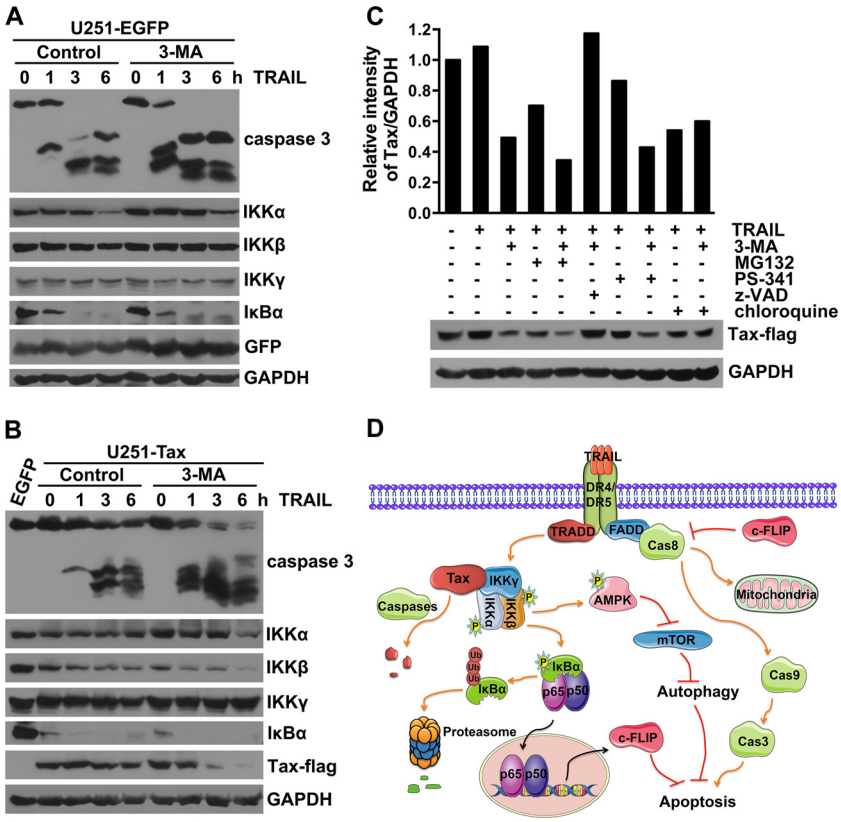

FIG 7 Inhibition of autophagy promotes TRAIL-induced Tax degradation. (A and B) 3-MA promotes TRAIL-induced degradation of Tax and IKKα/β. U251 cells were infected with LV-EGFP (A) or LV-Tax (B) for 4 days, pretreated without (control) or with 10 mM 3-MA for 3 h, and then treated with 50 ng/ml TRAIL for the indicated times. The caspase-3 activation and the expression levels of the IKK complex, IκBα, and Tax were determined using Western blot assays. (C) The pan-caspase inhibitor blocks the Tax degradation induced by the combination of 3-MA and TRAIL. U251 cells were infected with LV-Tax for 4 days, pretreated with or without 10 mM 3-MA, 50 μM MG-132, 1 mM PS-341, 10 μM z-VAD-fmk, or 200 μM chloroquine for 3 h, and then treated with 50 ng/ml TRAIL for 3 h. The level of Tax expression was analyzed using Western blot assays. Protein quantification was performed via densitometry, and the ratios of Tax to GAPDH are shown for the respective blots. (D) Summarized interactions between Tax, autophagy, and TRAIL-mediated apoptosis.

clin-1 or UVRAG small interfering RNAs in FLIP-overexpressing Hct116 and Jurkat cells and $Bax^{-/-}$ Hct116 cells initiates a caspase-8-dependent mitochondrial apoptotic response (69). Accordingly, in the present study, we observed that the TRAIL-induced activation of caspase-8 and -3 was suppressed in Tax-expressing U251 cells and the inhibition of autophagy using 3-MA enhanced the TRAIL-induced activation of caspase-8 and -3 (Fig. 3C) and reduced c-$FLIP_S$ expression as well (data not shown). These results indicate that TRAIL-mediated apoptosis could be regulated at the DISC level through the inhibition of autophagy, but the molecular mechanism underlying this regulation needs to be further explored.

Besides HTLV-1 Tax-induced resistance against apoptosis, Tax-mediated induction of apoptosis was also reported in previous investigation. For example, hormone-dependent activation of Tax resulted in an inhibition of cell proliferation and an apoptotic cell death in Jurkat T cells (70). Retrovirus-mediated Tax expression in Jurkat T cells was reported to induce apoptosis, which is mediated by NF-κB-activated expression of TRAIL (71). We examined the TRAIL mRNA expression in LV-Tax-infected U251 cells compared with LV-EGFP-infected ones, while IL-6 mRNA expression, which is reported to be increased in Tax-expressing U251 cells (9), was detected to confirm the function of Tax. Results showed that IL-6 mRNA was upregulated in Tax-expressing U251 cells, but the expression of TRAIL mRNA remains unchanged (data not shown). Therefore, we speculate that Tax affects apoptosis signaling specifically in different cell types.

Results of this study indicate that activation of NF-κB is required for Tax-induced c-FLIP expression in U251 cells. This result is consistent with previous studies conducted in HTLV-1-infected and Tax-expressing T cells (26). However, the mechanism by which Tax activates the autophagy pathway has not been clearly elucidated. Tang et al. indicated that HTLV-1 Tax induces autophagy by inhibition of autophagosome-lysosome fusion in HeLa cells, and the regulation of autophagy is correlated with the ability of Tax to activate NF-κB, because the Tax M22 mutant cannot increase autophagosome accumulation (41). Meanwhile, Ren et al. reported that HTLV-2 Tax induced autophagy by connecting the IKK complex to the autophagy pathway, and the complex contained Beclin1 and class III PI3K (42). Here, we demonstrate that Tax-induced autophagy and c-FLIP upregulation correlate with the ability of Tax to activate NF-κB. Our further analysis of the effects of key components in the Tax-induced NF-κB pathway on c-FLIP expression and autophagy activation demonstrates that the Tax-induced upregulation of c-FLIP requires the activation of both IKK and NF-κB, whereas Tax-induced autophagy is dependent upon the activation of IKK but not NF-κB. Recently, the IKK complex was shown to promote au-

tophagy in an NF-κB-independent manner in human and murine cells. In addition, the inhibition of mTOR and the activation of AMPK, which are strictly associated with starvation-induced autophagy, are both involved in this NF-κB-independent process (57). However, another report indicated that IKK-mediated autophagy involves IKK-dependent and NF-κB-independent increases in the expression of proautophagic genes (72). Although the detailed mechanism underlying IKK-induced autophagy is largely unknown, these results suggest that IKK-regulated autophagy does not require the activation of NF-κB. Therefore, we propose that Tax-induced autophagy involves the Tax-induced activation of the IKK complex and exhibits the same downstream signaling pathway as IKK-induced autophagy, because these two processes are both independent of NF-κB.

In the past, extensive studies focused on the mechanism by which Tax affects the cellular apoptosis or proliferation signals that aid HTLV-1 viral replication and escape. However, the mechanism through which cellular signaling regulates Tax stability has rarely been explored. It was recently reported that HTLV-1 Tax-increased autophagosome accumulation could modulate the degradation of Tax itself (41). We have observed that TRAIL-mediated apoptosis promotes Tax degradation, which could be further enhanced by the downregulation of c-FLIP expression or the inhibition of autophagy. In addition, TRAIL-induced degradation of IKKα and IKKβ, but not IKKγ, is observed in Tax-expressing cells. These results suggest that TRAIL may cause dissociation of the Tax-IKK complex and result in the degradation of Tax, IKKα, and IKKβ through a different mechanism. Ubiquitination has been shown to play a critical role in cellular localization and cellular functions, including the activation of NF-κB by HTLV-1 Tax (73, 74). Interestingly, recent reports have demonstrated that a newly identified ubiquitin E3 ligase, PDLIM2, can promote the K48-linked polyubiquitination of Tax and recruits Tax from the cytoplasm and Tax nuclear bodies into the nuclear matrix, where the polyubiquitinated Tax is degraded by the proteasome (75). Our analysis of the effects of inhibitors of the proteasome, lysosome, and caspases on Tax degradation indicates that only caspase inhibitors can suppress the Tax degradation induced by the combination of TRAIL and 3-MA. However, inhibitors of both the proteasome and the lysosome promote Tax degradation, likely because these inhibitors promote TRAIL-induced apoptosis. These data suggest that the activation of caspases induced by TRAIL may be responsible for the Tax degradation. Although there is no report showing that HTLV-1 Tax can be cleaved by caspases, several potential cleavage sites of caspases in the Tax protein sequence have been predicted; further experiments are needed to confirm these cleavage sites and explore the underlying mechanism of TRAIL-mediated Tax degradation.

In conclusion, we have shown that the HTLV-1 Tax protein inhibits death receptor-mediated apoptosis not only through the upregulation of c-FLIP expression but also via the activation of the autophagy pathway. In addition, inhibition of autophagy results in TRAIL-induced Tax degradation. These data indicate that investigating the regulation of apoptosis and autophagy mediated by Tax may aid in the development of novel therapeutic strategies for the treatment of HTLV-1 infection-related diseases through the inhibition of autophagy.

ACKNOWLEDGMENTS

This work was partially supported by the State Key Basic Research Program of China (grant no. 2007CB507404), the Natural Science Foundation of China (grant no. 30972684) and the Doctoral Degree Program of the Ministry of Education (grant no. 20101196110027).

We have no conflicts of interest to declare.

REFERENCES

1. **Osame M, Usuku K, Izumo S, Ijichi N, Amitani H, Igata A, Matsumoto M, Tara M.** 1986. HTLV-I associated myelopathy, a new clinical entity. Lancet **i:**1031–1032.
2. **Yoshida M.** 2005. Discovery of HTLV-1, the first human retrovirus, its unique regulatory mechanisms, and insights into pathogenesis. Oncogene **24:**5931–5937. http://dx.doi.org/10.1038/sj.onc.1208981.
3. **Giam CZ, Jeang KT.** 2007. HTLV-1 Tax and adult T-cell leukemia. Front. Biosci. **12:**1496–1507. http://dx.doi.org/10.2741/2163.
4. **Nagai M, Osame M.** 2003. Human T-cell lymphotropic virus type I and neurological diseases. J. Neurovirol. **9:**228–235. http://dx.doi.org/10.1080/13550280390194028.
5. **Goncalves DU, Proietti FA, Barbosa-Stancioli EF, Martins ML, Ribas JG, Martins-Filho OA, Teixeira-Carvalho A, Peruhype-Magalhaes V, Carneiro-Proietti AB.** 2008. HTLV-1-associated myelopathy/tropical spastic paraparesis (HAM/TSP) inflammatory network. Inflamm. Allergy Drug Targets **7:**98–107. http://dx.doi.org/10.2174/187152808785107642.
6. **Lepoutre V, Jain P, Quann K, Wigdahl B, Khan ZK.** 2009. Role of resident CNS cell populations in HTLV-1-associated neuroinflammatory disease. Front. Biosci. **14:**1152–1168. http://dx.doi.org/10.2741/3300.
7. **Lehky TJ, Fox CH, Koenig S, Levin MC, Flerlage N, Izumo S, Sato E, Raine CS, Osame M, Jacobson S.** 1995. Detection of human T-lymphotropic virus type I (HTLV-I) tax RNA in the central nervous system of HTLV-I-associated myelopathy/tropical spastic paraparesis patients by in situ hybridization. Ann. Neurol. **37:**167–175. http://dx.doi.org/10.1002/ana.410370206.
8. **Giraudon P, Malcus C, Chalon A, Vincent P, Khuth S, Bernard A, Belin MF.** 2003. Astrocytes, cells involved in neuro-immune interactions in the central nervous system. J. Soc. Biol. **197:**103–112. (In French.)
9. **Banerjee P, Rochford R, Antel J, Canute G, Wrzesinski S, Sieburg M, Feuer G.** 2007. Proinflammatory cytokine gene induction by human T-cell leukemia virus type 1 (HTLV-1) and HTLV-2 Tax in primary human glial cells. J. Virol. **81:**1690–1700. http://dx.doi.org/10.1128/JVI.01513-06.
10. **Jin Q, Alkhatib B, Cornetta K, Alkhatib G.** 2010. Alternate receptor usage of neuropilin-1 and glucose transporter protein 1 by the human T cell leukemia virus type 1. Virology **396:**203–212. http://dx.doi.org/10.1016/j.virol.2009.10.015.
11. **Yoshida M.** 1993. HTLV-1 Tax: regulation of gene expression and disease. Trends Microbiol. **1:**131–135. http://dx.doi.org/10.1016/0966-842X(93)90127-D.
12. **Tanaka A, Takahashi C, Yamaoka S, Nosaka T, Maki M, Hatanaka M.** 1990. Oncogenic transformation by the tax gene of human T-cell leukemia virus type I in vitro. Proc. Natl. Acad. Sci. U. S. A. **87:**1071–1075. http://dx.doi.org/10.1073/pnas.87.3.1071.
13. **Jeang KT, Giam CZ, Majone F, Aboud M.** 2004. Life, death, and tax: role of HTLV-I oncoprotein in genetic instability and cellular transformation. J. Biol. Chem. **279:**31991–31994. http://dx.doi.org/10.1074/jbc.R400009200.
14. **Taylor JM, Nicot C.** 2008. HTLV-1 and apoptosis: role in cellular transformation and recent advances in therapeutic approaches. Apoptosis **13:**733–747. http://dx.doi.org/10.1007/s10495-008-0208-7.
15. **Liu M, Yang L, Zhang L, Liu B, Merling R, Xia Z, Giam CZ.** 2008. Human T-cell leukemia virus type 1 infection leads to arrest in the G_1 phase of the cell cycle. J. Virol. **82:**8442–8455. http://dx.doi.org/10.1128/JVI.00091-08.
16. **Yang L, Kotomura N, Ho YK, Zhi H, Bixler S, Schell MJ, Giam CZ.** 2011. Complex cell cycle abnormalities caused by human T-lymphotropic virus type 1 Tax. J. Virol. **85:**3001–3009. http://dx.doi.org/10.1128/JVI.00086-10.
17. **Huang J, Ren T, Guan H, Jiang Y, Cheng H.** 2009. HTLV-1 Tax is a critical lipid raft modulator that hijacks IkappaB kinases to the microdomains for persistent activation of NF-kappaB. J. Biol. Chem. **284:**6208–6217. http://dx.doi.org/10.1074/jbc.M806390200.
18. **Grassmann R, Aboud M, Jeang KT.** 2005. Molecular mechanisms of cellular transformation by HTLV-1 Tax. Oncogene **24:**5976–5985. http://dx.doi.org/10.1038/sj.onc.1208978.
19. **Harhaj EW, Harhaj NS.** 2005. Mechanisms of persistent NF-kappaB

activation by HTLV-I tax. IUBMB Life **57:**83–91. http://dx.doi.org/10.1080/15216540500078715.
20. **Qu Z, Xiao G.** 2011. Human T-cell lymphotropic virus: a model of NF-kappaB-associated tumorigenesis. Viruses **3:**714–749. http://dx.doi.org/10.3390/v3060714.
21. **Matsuoka M, Jeang KT.** 2007. Human T-cell leukaemia virus type 1 (HTLV-1) infectivity and cellular transformation. Nat. Rev. Cancer **7:**270–280. http://dx.doi.org/10.1038/nrc2111.
22. **Yamaoka S, Inoue H, Sakurai M, Sugiyama T, Hazama M, Yamada T, Hatanaka M.** 1996. Constitutive activation of NF-kappa B is essential for transformation of rat fibroblasts by the human T-cell leukemia virus type I Tax protein. EMBO J. **15:**873–887.
23. **Park HU, Jeong SJ, Jeong JH, Chung JH, Brady JN.** 2006. Human T-cell leukemia virus type 1 Tax attenuates gamma-irradiation-induced apoptosis through physical interaction with Chk2. Oncogene **25:**438–447. http://dx.doi.org/10.1038/sj.onc.1209059.
24. **Stoppa G, Rumiato E, Saggioro D.** 2012. Ras signaling contributes to survival of human T-cell leukemia/lymphoma virus type 1 (HTLV-1) Tax-positive T-cells. Apoptosis **17:**219–228. http://dx.doi.org/10.1007/s10495-011-0676-z.
25. **Krueger A, Fas SC, Giaisi M, Bleumink M, Merling A, Stumpf C, Baumann S, Holtkotte D, Bosch V, Krammer PH, Li-Weber M.** 2006. HTLV-1 Tax protects against CD95-mediated apoptosis by induction of the cellular FLICE-inhibitory protein (c-FLIP). Blood **107:**3933–3939. http://dx.doi.org/10.1182/blood-2005-06-2567.
26. **Okamoto K, Fujisawa J, Reth M, Yonehara S.** 2006. Human T-cell leukemia virus type-I oncoprotein Tax inhibits Fas-mediated apoptosis by inducing cellular FLIP through activation of NF-kappaB. Genes Cells **11:**177–191. http://dx.doi.org/10.1111/j.1365-2443.2006.00927.x.
27. **Matsuda T, Almasan A, Tomita M, Uchihara JN, Masuda M, Ohshiro K, Takasu N, Yagita H, Ohta T, Mori N.** 2005. Resistance to Apo2 ligand (Apo2L)/tumor necrosis factor-related apoptosis-inducing ligand (TRAIL)-mediated apoptosis and constitutive expression of Apo2L/TRAIL in human T-cell leukemia virus type 1-infected T-cell lines. J. Virol. **79:**1367–1378. http://dx.doi.org/10.1128/JVI.79.3.1367-1378.2005.
28. **Wiley SR, Schooley K, Smolak PJ, Din WS, Huang CP, Nicholl JK, Sutherland GR, Smith TD, Rauch C, Smith CA, Goodwin RG.** 1995. Identification and characterization of a new member of the TNF family that induces apoptosis. Immunity **3:**673–682. http://dx.doi.org/10.1016/1074-7613(95)90057-8.
29. **Schneider P, Thome M, Burns K, Bodmer JL, Hofmann K, Kataoka T, Holler N, Tschopp J.** 1997. TRAIL receptors 1 (DR4) and 2 (DR5) signal FADD-dependent apoptosis and activate NF-kappaB. Immunity **7:**831–836. http://dx.doi.org/10.1016/S1074-7613(00)80401-X.
30. **Gonzalvez F, Ashkenazi A.** 2010. New insights into apoptosis signaling by Apo2L/TRAIL. Oncogene **29:**4752–4765. http://dx.doi.org/10.1038/onc.2010.221.
31. **Mahalingam D, Szegezdi E, Keane M, de Jong S, Samali A.** 2009. TRAIL receptor signalling and modulation: are we on the right TRAIL? Cancer Treat. Rev. **35:**280–288. http://dx.doi.org/10.1016/j.ctrv.2008.11.006.
32. **Irmler M, Thome M, Hahne M, Schneider P, Hofmann K, Steiner V, Bodmer JL, Schroter M, Burns K, Mattmann C, Rimoldi D, French LE, Tschopp J.** 1997. Inhibition of death receptor signals by cellular FLIP. Nature **388:**190–195. http://dx.doi.org/10.1038/40657.
33. **Panka DJ, Mano T, Suhara T, Walsh K, Mier JW.** 2001. Phosphatidylinositol 3-kinase/Akt activity regulates c-FLIP expression in tumor cells. J. Biol. Chem. **276:**6893–6896. http://dx.doi.org/10.1074/jbc.C000569200.
34. **Yeh JH, Hsu SC, Han SH, Lai MZ.** 1998. Mitogen-activated protein kinase kinase antagonized fas-associated death domain protein-mediated apoptosis by induced FLICE-inhibitory protein expression. J. Exp. Med. **188:**1795–1802. http://dx.doi.org/10.1084/jem.188.10.1795.
35. **Micheau O, Lens S, Gaide O, Alevizopoulos K, Tschopp J.** 2001. NF-kappaB signals induce the expression of c-FLIP. Mol. Cell. Biol. **21:**5299–5305. http://dx.doi.org/10.1128/MCB.21.16.5299-5305.2001.
36. **Bleumink M, Kohler R, Giaisi M, Proksch P, Krammer PH, Li-Weber M.** 2011. Rocaglamide breaks TRAIL resistance in HTLV-1-associated adult T-cell leukemia/lymphoma by translational suppression of c-FLIP expression. Cell Death Differ. **18:**362–370. http://dx.doi.org/10.1038/cdd.2010.99.
37. **Levine B, Kroemer G.** 2008. Autophagy in the pathogenesis of disease. Cell **132:**27–42. http://dx.doi.org/10.1016/j.cell.2007.12.018.
38. **Klionsky DJ.** 2007. Autophagy: from phenomenology to molecular understanding in less than a decade. Nat. Rev. Mol. Cell Biol. **8:**931–937. http://dx.doi.org/10.1038/nrm2245.
39. **Jung CH, Ro SH, Cao J, Otto NM, Kim DH.** 2010. mTOR regulation of autophagy. FEBS Lett. **584:**1287–1295. http://dx.doi.org/10.1016/j.febslet.2010.01.017.
40. **Tanida I, Ueno T, Kominami E.** 2008. LC3 and autophagy. Methods Mol. Biol. **445:**77–88. http://dx.doi.org/10.1007/978-1-59745-157-4_4.
41. **Tang SW, Chen CY, Klase Z, Zane L, Jeang KT.** 2013. The cellular autophagy pathway modulates HTLV-1 replication. J. Virol. **87:**1699–1707. http://dx.doi.org/10.1128/JVI.02147-12.
42. **Ren T, Dong W, Takahashi Y, Xiang D, Yuan Y, Liu X, Loughran TP, Jr, Sun SC, Wang HG, Cheng H.** 2012. HTLV-2 Tax immortalizes human CD4+ memory T lymphocytes by oncogenic activation and dysregulation of autophagy. J. Biol. Chem. **287:**34683–34693. http://dx.doi.org/10.1074/jbc.M112.377143.
43. **Guo Y, Chen C, Zheng Y, Zhang J, Tao X, Liu S, Zheng D, Liu Y.** 2005. A novel anti-human DR5 monoclonal antibody with tumoricidal activity induces caspase-dependent and caspase-independent cell death. J. Biol. Chem. **280:**41940–41952. http://dx.doi.org/10.1074/jbc.M503621200.
44. **Lum JJ, Bauer DE, Kong M, Harris MH, Li C, Lindsten T, Thompson CB.** 2005. Growth factor regulation of autophagy and cell survival in the absence of apoptosis. Cell **120:**237–248. http://dx.doi.org/10.1016/j.cell.2004.11.046.
45. **Amaravadi RK, Yu D, Lum JJ, Bui T, Christophorou MA, Evan GI, Thomas-Tikhonenko A, Thompson CB.** 2007. Autophagy inhibition enhances therapy-induced apoptosis in a Myc-induced model of lymphoma. J. Clin. Invest. **117:**326–336. http://dx.doi.org/10.1172/JCI28833.
46. **Corcelle EA, Puustinen P, Jäättelä M.** 2009. Apoptosis and autophagy: targeting autophagy signalling in cancer cells—'trick or treats'? FEBS J. **276:**6084–6096. http://dx.doi.org/10.1111/j.1742-4658.2009.07332.x.
47. **Hou W, Han J, Lu C, Goldstein LA, Rabinowich H.** 2008. Enhancement of tumor-TRAIL susceptibility by modulation of autophagy. Autophagy **4:**940–943.
48. **Maiuri MC, Zalckvar E, Kimchi A, Kroemer G.** 2007. Self-eating and self-killing: crosstalk between autophagy and apoptosis. Nat. Rev. Mol. Cell Biol. **8:**741–752. http://dx.doi.org/10.1038/nrm2239.
49. **Liang XH, Jackson S, Seaman M, Brown K, Kempkes B, Hibshoosh H, Levine B.** 1999. Induction of autophagy and inhibition of tumorigenesis by beclin 1. Nature **402:**672–676. http://dx.doi.org/10.1038/45257.
50. **Boya P, Gonzalez-Polo RA, Casares N, Perfettini JL, Dessen P, Larochette N, Metivier D, Meley D, Souquere S, Yoshimori T, Pierron G, Codogno P, Kroemer G.** 2005. Inhibition of macroautophagy triggers apoptosis. Mol. Cell. Biol. **25:**1025–1040. http://dx.doi.org/10.1128/MCB.25.3.1025-1040.2005.
51. **Chang DW, Xing Z, Pan Y, Algeciras-Schimnich A, Barnhart BC, Yaish-Ohad S, Peter ME, Yang X.** 2002. c-FLIP(L) is a dual function regulator for caspase-8 activation and CD95-mediated apoptosis. EMBO J. **21:**3704–3714. http://dx.doi.org/10.1093/emboj/cdf356.
52. **Neumann L, Pforr C, Beaudouin J, Pappa A, Fricker N, Krammer PH, Lavrik IN, Eils R.** 2010. Dynamics within the CD95 death-inducing signaling complex decide life and death of cells. Mol. Syst. Biol. **6:**352. http://dx.doi.org/10.1038/msb.2010.6.
53. **Azran I, Schavinsky-Khrapunsky Y, Aboud M.** 2004. Role of Tax protein in human T-cell leukemia virus type-I leukemogenicity. Retrovirology **1:**20. http://dx.doi.org/10.1186/1742-4690-1-20.
54. **Saggioro D.** 2011. Anti-apoptotic effect of Tax: an NF-kappaB path or a CREB way? Viruses **3:**1001–1014. http://dx.doi.org/10.3390/v3071001.
55. **Smith MR, Greene WC.** 1990. Identification of HTLV-I tax trans-activator mutants exhibiting novel transcriptional phenotypes. Genes Dev. **4:**1875–1885. http://dx.doi.org/10.1101/gad.4.11.1875.
56. **Meley D, Bauvy C, Houben-Weerts JH, Dubbelhuis PF, Helmond MT, Codogno P, Meijer AJ.** 2006. AMP-activated protein kinase and the regulation of autophagic proteolysis. J. Biol. Chem. **281:**34870–34879. http://dx.doi.org/10.1074/jbc.M605488200.
57. **Criollo A, Senovilla L, Authier H, Maiuri MC, Morselli E, Vitale I, Kepp O, Tasdemir E, Galluzzi L, Shen S, Tailler M, Delahaye N, Tesniere A, De Stefano D, Younes AB, Harper F, Pierron G, Lavandero S, Zitvogel L, Israel A, Baud V, Kroemer G.** 2010. The IKK complex contributes to the induction of autophagy. EMBO J. **29:**619–631. http://dx.doi.org/10.1038/emboj.2009.364.
58. **Harhaj EW, Sun SC.** 1999. IKKgamma serves as a docking subunit of the IkappaB kinase (IKK) and mediates interaction of IKK with the human

T-cell leukemia virus Tax protein. J. Biol. Chem. **274:**22911–22914. http://dx.doi.org/10.1074/jbc.274.33.22911.
59. **Sir D, Ou JH.** 2010. Autophagy in viral replication and pathogenesis. Mol. Cells **29:**1–7. http://dx.doi.org/10.1007/s10059-010-0014-2.
60. **Wang X, Gao Y, Tan J, Devadas K, Ragupathy V, Takeda K, Zhao J, Hewlett I.** 2012. HIV-1 and HIV-2 infections induce autophagy in Jurkat and CD4+ T cells. Cell Signal. **24:**1414–1419. http://dx.doi.org/10.1016/j.cellsig.2012.02.016.
61. **Takahashi MN, Jackson W, Laird DT, Culp TD, Grose C, Haynes JI, II, Benetti L.** 2009. Varicella-zoster virus infection induces autophagy in both cultured cells and human skin vesicles. J. Virol. **83:**5466–5476. http://dx.doi.org/10.1128/JVI.02670-08.
62. **Law AH, Lee DC, Yuen KY, Peiris M, Lau AS.** 2010. Cellular response to influenza virus infection: a potential role for autophagy in CXCL10 and interferon-alpha induction. Cell Mol. Immunol. **7:**263–270. http://dx.doi.org/10.1038/cmi.2010.25.
63. **Tsukahara T, Kannagi M, Ohashi T, Kato H, Arai M, Nunez G, Iwanaga Y, Yamamoto N, Ohtani K, Nakamura M, Fujii M.** 1999. Induction of Bcl-x(L) expression by human T-cell leukemia virus type 1 Tax through NF-kappaB in apoptosis-resistant T-cell transfectants with Tax. J. Virol. **73:**7981–7987.
64. **Kanzawa T, Germano IM, Komata T, Ito H, Kondo Y, Kondo S.** 2004. Role of autophagy in temozolomide-induced cytotoxicity for malignant glioma cells. Cell Death Differ. **11:**448–457. http://dx.doi.org/10.1038/sj.cdd.4401359.
65. **Li J, Qin Z, Liang Z.** 2009. The prosurvival role of autophagy in Resveratrol-induced cytotoxicity in human U251 glioma cells. BMC Cancer **9:**215. http://dx.doi.org/10.1186/1471-2407-9-215.
66. **Nishikawa T, Tsuno NH, Okaji Y, Shuno Y, Sasaki K, Hongo K, Sunami E, Kitayama J, Takahashi K, Nagawa H.** 2010. Inhibition of autophagy potentiates sulforaphane-induced apoptosis in human colon cancer cells. Ann. Surg. Oncol. **17:**592–602. http://dx.doi.org/10.1245/s10434-009-0696-x.
67. **Mills KR, Reginato M, Debnath J, Queenan B, Brugge JS.** 2004. Tumor necrosis factor-related apoptosis-inducing ligand (TRAIL) is required for induction of autophagy during lumen formation in vitro. Proc. Natl. Acad. Sci. U. S. A. **101:**3438–3443. http://dx.doi.org/10.1073/pnas.0400443101.
68. **Herrero-Martin G, Hoyer-Hansen M, Garcia-Garcia C, Fumarola C, Farkas T, Lopez-Rivas A, Jaattela M.** 2009. TAK1 activates AMPK-dependent cytoprotective autophagy in TRAIL-treated epithelial cells. EMBO J. **28:**677–685. http://dx.doi.org/10.1038/emboj.2009.8.
69. **Han J, Hou W, Goldstein LA, Lu C, Stolz DB, Yin XM, Rabinowich H.** 2008. Involvement of protective autophagy in TRAIL resistance of apoptosis-defective tumor cells. J. Biol. Chem. **283:**19665–19677. http://dx.doi.org/10.1074/jbc.M710169200.
70. **Chlichlia K, Moldenhauer G, Daniel PT, Busslinger M, Gazzolo L, Schirrmacher V, Khazaie K.** 1995. Immediate effects of reversible HTLV-1 tax function: T-cell activation and apoptosis. Oncogene **10:**269–277.
71. **Rivera-Walsh I, Waterfield M, Xiao G, Fong A, Sun SC.** 2001. NF-kappaB signaling pathway governs TRAIL gene expression and human T-cell leukemia virus-I Tax-induced T-cell death. J. Biol. Chem. **276:**40385–40388. http://dx.doi.org/10.1074/jbc.C100501200.
72. **Comb WC, Cogswell P, Sitcheran R, Baldwin AS.** 2011. IKK-dependent, NF-kappaB-independent control of autophagic gene expression. Oncogene **30:**1727–1732. http://dx.doi.org/10.1038/onc.2010.553.
73. **Shibata Y, Tanaka Y, Gohda J, Inoue J.** 2011. Activation of the IkappaB kinase complex by HTLV-1 Tax requires cytosolic factors involved in Tax-induced polyubiquitination. J. Biochem. **150:**679–686. http://dx.doi.org/10.1093/jb/mvr106.
74. **Kfoury Y, Setterblad N, El-Sabban M, Zamborlini A, Dassouki Z, El Hajj H, Hermine O, Pique C, de The H, Saib A, Bazarbachi A.** 2011. Tax ubiquitylation and SUMOylation control the dynamic shuttling of Tax and NEMO between Ubc9 nuclear bodies and the centrosome. Blood **117:**190–199. http://dx.doi.org/10.1182/blood-2010-05-285742.
75. **Fu J, Yan P, Li S, Qu Z, Xiao G.** 2010. Molecular determinants of PDLIM2 in suppressing HTLV-I Tax-mediated tumorigenesis. Oncogene **29:**6499–6507. http://dx.doi.org/10.1038/onc.2010.374.